Effective Capacity of a Correlated Rayleigh Fading Channel

Qing Wang, Dapeng Wu and Pingyi Fan

Abstract

The next generation wireless networks call for quality of service (QoS) support. The effective capacity (EC) proposed by Wu and Negi provides a powerful tool for the design of QoS provisioning mechanisms. In their previous work, Wu and Negi derived a formula for effective capacity of a Rayleigh fading channel with arbitrary Doppler spectrum. However, their paper did not provide simulation results to verify the accuracy of the EC formula derived in their paper. This is due to difficulty in simulating a Rayleigh fading channel with a Doppler spectrum of continuous frequency, required by the EC formula. To address this difficulty, we develop a verification methodology based on a new discrete-frequency EC formula; different from the EC formula developed by Wu and Negi, our new discrete-frequency EC formula can be used in practice. Through simulation, we verify that the EC formula developed by Wu and Negi is accurate. Furthermore, to facilitate the application of the EC theory to the design of practical QoS provisioning mechanisms in wireless networks, we propose a spectral-estimation-based algorithm to estimate the EC function, given channel measurements; we also analyze the effect of spectral estimation error on the accuracy of EC estimation. Simulation results show that our proposed spectral-estimation-based EC estimation algorithm is accurate, indicating the excellent practicality of our algorithm.

Index Terms

Effective capacity, Rayleigh fading, Doppler spectrum, QoS provisioning.

I. Introduction

A. Review of Effective Capacity

Future wireless networks are expected to provide quality of service (QoS). The effective capacity (EC) proposed by Wu and Negi [1] provides a powerful tool for the design of QoS provisioning mechanisms since the effective capacity approach provides a simple and accurate method for predicting link-layer QoS performance measures such as data rate, delay, and delay bound violation probability. Effective capacity

Qing Wang and Pingyi Fan are with Tsinghua University, Beijing, P. R. China. Dapeng Wu is with Department of Electrical and Computer Engineering, University of Florida, Gainesville, FL 32611. Correspondence author: Prof. Dapeng Wu, wu@ece.ufl.edu, http://www.wu.ece.ufl.edu.

is a link-layer model in which a wireless link is modeled by two EC functions, namely the probability $\gamma(\mu)$ of nonempty buffer and the QoS exponent $\theta(\mu)$ of a connection. Both of them are functions of the source traffic rate μ. The parsimonious EC channel model characterizes the capacity of a fading channel; mathematically, it is the dual of the effective bandwidth function [2], which characterizes the source randomness. Specifically, the key point in the theory of effective capacity is that for a source that requires a communication delay bound D_{max} and can tolerate a delay-bound violation probability not more than ε, we need to limit its data rate, i.e., the maximum data rate is μ, where μ is the solution to $\varepsilon = \gamma(\mu)e^{-\theta(\mu)D_{max}}$, in which $\theta(\mu) = \mu\alpha^{-1}(\mu)$. Here $\alpha^{-1}(\cdot)$ is the inverse function of the effective capacity function $\alpha(\cdot)$. Next we review the definition of effective capacity.

Let $r(t)$ be the instantaneous channel capacity at time t. Define $S(t) = \int_0^t r(\tau)d\tau$, which is the service provided by the channel during the interval $[0, t]$. Suppose the stochastic process $r(t)$ is ergodic and stationary. Then the effective capacity function of $r(t)$ is defined by

$$\alpha(u) = \frac{-\Lambda(-u)}{u}, \ \ \forall u > 0, \tag{1}$$

where

$$\Lambda(-u) = \lim_{t\to\infty} \frac{1}{t} \log E[e^{-uS(t)}]. \tag{2}$$

Thus if we know the effective capacity $\alpha(u)$, we can derive the QoS exponent function $\theta(\cdot)$; then, given the communication delay bound D_{max} and a delay-bound violation probability ε, we can estimate the probability $\gamma(\mu)$ of nonempty buffer and constrain the source rate μ to satisfy the requested delay-bound violation probability.

B. Motivation of our work

EC theory is an effective approach to the design of QoS provisioning mechanisms which has attracted considerable attention recently. Since Wu and Negi proposed it in 2003 [1], the EC approach has been widely applied to various wireless systems and applications, e.g., multiple-input-multiple-output (MIMO) systems [3], adaptive-modulation-and-coding and power control [4], amplify-and-forward and decode-and-forward relay networks (cooperative diversity) [5], resource allocation [6], arbitrary time scale in Nakagami-m fading channels [7], maximum quantile scheduling [8], joint design of video compression, link layer and physical layer [9], study of joint impact of bandwidth, power, and code-rate on the effective

capacity [10], and multi-hop delay performance in wireless mesh networks [11]. However, most EC-related works only considered i.i.d. Rayleigh fading channels due to difficulty in analyzing the EC of non-i.i.d. Rayleigh fading channels. Although Wu and Negi [1] derived a formula for effective capacity of a Rayleigh fading channel with arbitrary Doppler spectrum, no one has verified the accuracy of the EC formula. This is due to difficulty in simulating a Rayleigh fading channel with a Doppler spectrum of continuous frequency, required by the EC formula. It is important to verify the accuracy of the EC formula because its accurateness will allow researchers to use the EC formula to study the systems under non-i.i.d. Rayleigh fading channels, instead of i.i.d. Rayleigh fading channels only.

Since we can only simulate a discrete-time system, we are not able to directly verify the accuracy of the EC formula of a Rayleigh fading channel with a Doppler spectrum of continuous frequency. Instead, we propose a new formula for the EC function in terms of discrete frequency; then we only need to verify the accuracy of the discrete-frequency formula for the EC function, through simulations. As long as the sampling interval in frequency Δf_s is sufficiently small, the accuracy of the discrete-frequency formula for the EC function is equivalent to the continuous-frequency formula for the EC function. Based on this idea, we develop a verification methodology, the details of which is given in Section III. We implement the verification methodology and conduct simulations. Our simulation results agree very well with the discrete-frequency formula of the EC function for sufficiently small Δf_s. Hence, for the first time, we verify that the EC formula given in Ref. [1] is accurate.

In practice, we cannot directly use the formula of the EC function to compute the effective capacity since the power spectral density of the fading channel is not given *a priori*; in other words, we need to estimate the power spectral density of the fading channel in order to use the formula of the EC function. Therefore, to facilitate the application of the EC theory to the design of practical QoS provisioning mechanisms in wireless networks, we propose a spectral-estimation-based algorithm to estimate the EC function, given channel measurements. In addition, we analyze the effect of spectral estimation error on the accuracy of EC estimation. Simulation results show that our proposed spectral-estimation-based EC estimation algorithm is accurate, indicating the excellent practicality of our algorithm.

The rest of the paper is organized as follows. In Section II, we review the key steps in the derivation of the EC formula for a Rayleigh fading channel with arbitrary Doppler spectrum [1], and propose a discrete-frequency formula for the EC function. In Section III, we propose a methodology to verify the

accuracy of the EC formula. In Section IV, we propose a spectral-estimation-based algorithm to estimate the EC function for practical use of the EC theory, and analyze the effect of spectral estimation error on the accuracy of EC estimation. Section V shows the simulation results, which verify that the EC formula in Ref. [1] is accurate, and our proposed spectral-estimation-based EC estimation algorithm is also accurate. Section VI concludes the paper.

II. Derivation of Effective Capacity of a Correlated Rayleigh Fading Channel

In this section, we review the key steps in the derivation of the EC formula for a correlated Rayleigh fading channel in Wu and Negi's work [1].

Suppose that the wireless channel is a Rayleigh flat fading channel in AWGN with Doppler spectrum $S(f)$. Assume that we have perfect causal knowledge of the channel gains. We show how to calculate the effective capacity for this channel. Denote a sequence of N_t measurements of the channel gain over the duration $[0, t]$, spaced at a time-interval δ apart, by $\mathbf{x} = [x(0), x(1), \cdots, x(N_t - 1)]^T$, where $x(n)$ $(n = 0, 1, \cdots, N_t - 1)$ are the complex-valued channel gains ($|x(n)|$ are therefore Rayleigh distributed) and $[\cdot]^T$ is a transpose operation. Without loss of generality, we have absorbed the noise variance into the definition of $x(n)$. That is, the channel gain is scaled so that the noise variance is always normalized to 1. The measurement $x(n)$ is a realization of a random variable sequence denoted by $X(n)$, which can be written as the vector $\mathbf{X} = [X(0), X(1), \cdots, X(N_t - 1)]^T$. The PDF of a random vector $\mathbf{X}$ for the Rayleigh fading channel is

$$f_{\mathbf{X}}(\mathbf{x}) = \frac{1}{\pi^{N_t} det(\mathbf{R})} e^{-\mathbf{x}^H \mathbf{R}^{-1} \mathbf{x}}, \tag{3}$$

where $\mathbf{R}$ is the covariance matrix of the random vector $\mathbf{X}$, $det(\mathbf{R})$ the determinant of matrix $\mathbf{R}$, and $\mathbf{x}^H$ the conjugate transpose of $\mathbf{x}$. According to (1) and (2), to calculate the EC function, we need to know

the expression of $E[e^{-uS(t)}]$; we derive it as below

$$\begin{aligned} E[e^{-uS(t)}] &= E[e^{-u\int_0^t r(\tau)d\tau}] \\ &\approx \int e^{-u(\sum_{i=1}^{n}\delta\times r(\tau_i))} f_{\mathbf{X}}(\mathbf{x})d\mathbf{x} \\ &= \int e^{-u(\sum_{i=1}^{n}\delta\times \log(1+|x(i)|^2))} f_{\mathbf{X}}(\mathbf{x})d\mathbf{x} \\ &\overset{(a)}{\approx} \int e^{-u\delta(\sum_{i=1}^{n}|x(i)|^2)} f_{\mathbf{X}}(\mathbf{x})d\mathbf{x} \\ &= \int e^{-u\delta(\sum_{i=1}^{n}||\mathbf{x}||^2)} \frac{1}{\pi^N \det(\mathbf{R})} e^{-\mathbf{x}^H\mathbf{R}^{-1}\mathbf{x}} d\mathbf{x} \\ &= \frac{1}{\pi^n \det(\mathbf{R})} \int e^{-\mathbf{x}^H(\mathbf{R}^{-1}+u\delta\mathbf{I})\mathbf{x}} d\mathbf{x} \\ &= \frac{1}{\pi^n \det(\mathbf{R})} \times \pi^n \det((\mathbf{R}^{-1}+u\delta\mathbf{I})^{-1}) \\ &= \frac{1}{\det(u\delta\mathbf{R}+\mathbf{I})} \end{aligned} \tag{4}$$

Note that the approximation, i.e., $\log(1+|x|^2) \approx |x|^2$, is used in (a). Thus, the derived formula is accurate for low signal-to-noise ratio (SNR) but is inaccurate for high SNR.

Denote the eigenvalues of matrix $\mathbf{R}$ by λ_n $(n = 1, 2, \cdots, N_t)$. Since $\mathbf{R}$ is symmetric, we have $\mathbf{R} = \mathbf{U}\mathbf{\Sigma}\mathbf{U}^H$, where $\mathbf{U}$ is a unitary matrix; $\mathbf{U}^H$ is its Hermitian; and the diagonal matrix $\mathbf{\Sigma} = diag(\lambda_1, \lambda_2, \cdots, \lambda_{N_t})$.

From (4), we have

$$\begin{aligned} E[e^{-uS(t)}] &\approx \frac{1}{\det(u\delta\mathbf{R}+\mathbf{I})} \\ &= \frac{1}{\det(u\delta\mathbf{U}\mathbf{\Sigma}\mathbf{U}^H + \mathbf{U}\mathbf{U}^H)} \\ &= \frac{1}{\det(\mathbf{U}diag(u\delta\lambda_1+1, \cdots, u\delta\lambda_{N_t}+1)\mathbf{U}^H)} \\ &= \frac{1}{\prod_{i=1}^{N_t}(u\delta\lambda_i+1)} \\ &= e^{-\sum_{i=1}^{N_t}\log(u\delta\lambda_i+1)} \end{aligned} \tag{5}$$

Plugging (5) into (2), we have

$$\begin{aligned}
\Lambda(-u) &\approx \lim_{t\to\infty} \frac{1}{t} \log e^{-\sum_{i=1}^{N_t} \log(u\delta\lambda_i+1)} \\
&= \lim_{N_t\to\infty} \frac{1}{(N_t-1)\delta} \log e^{-\sum_{i=1}^{N_t} \log(u\delta\lambda_i+1)} \\
&\overset{(a)}{=} \lim_{\Delta f\to 0} -\Delta f \sum_{i=1}^{N_t} \log(u\frac{\lambda_i}{B_w}+1) \qquad (6) \\
&\overset{(b)}{=} \lim_{\Delta f\to 0} -\sum_{i=1}^{N_t} \log(uS(f_i)+1)\Delta f \qquad (7) \\
&\overset{(c)}{=} -\int \log(uS(f)+1)df \qquad (8)
\end{aligned}$$

where (a) follows from the fact that the frequency interval $\Delta f = 1/t = \frac{1}{(N_t-1)\delta}$ and the bandwidth $B_w = 1/\delta$, (b) from the fact that the power spectral density $S(f_i) = \lambda_i/B_w$, and (c) from the fact that the limit of a sum becomes an integral, and $\Delta f \to 0$ implies $N_t \to \infty$ since $\Delta f = \frac{1}{(N_t-1)\delta}$. Note that $S(f)$ is the continuous-frequency power spectral density of the channel gain process and $S(f_i) = \lambda_i/B_w$ is the corresponding discrete-frequency power spectral density.

We can see that (8) in continuous form is the limit of (7) in discrete form when the sampling interval in frequency Δf goes to zero. Hence, from (1), (2), and (7), we obtain a discrete-form formula for the EC function, denoted by $\alpha^{(d)}(u)$, as below

$$\alpha^{(d)}(u) = \frac{\sum_{i=1}^{N_f} \log(uS(f_i)+1)\Delta f_s}{u}, \ u > 0, \qquad (9)$$

where N_f is the number of samples; $\Delta f_s = 2 \times f_m/(N_f - 1)$, where f_m is the maximum Doppler frequency of the fading channel. In practice, we can use discrete Fourier transform (DFT) to estimate the power spectral density $\{S(f_i)\}$ and the spectral span is $2 \times f_m$, which includes both positive and negative frequency; hence, given N_f samples, the resolution in frequency is $\Delta f_s = 2 \times f_m/(N_f - 1)$.

From (1), (2), and (8), we obtain a continuous-form formula for the EC function, denoted by $\alpha^{(c)}(u)$, as below

$$\alpha^{(c)}(u) = \frac{\int \log(uS(f)+1)df}{u}, \ u > 0. \qquad (10)$$

(10) was given in Ref. [1] while (9) is only given in this paper.

III. Methodology for Verifying the Accuracy of the EC Formula of Wu and Negi

In this section, we present a methodology to verify the accuracy of the EC formula (10) given in Ref. [1].

Since we can only simulate a discrete-time system, hence we can only verify the accuracy of the discrete-form formula for the EC function $\alpha^{(d)}(u)$ in (9). From (7), if Δf_s is sufficiently small, we have $\alpha^{(d)}(u) \approx \alpha^{(c)}(u)$. Hence, as long as we choose sufficiently small Δf_s, we are able to verify the accuracy of $\alpha^{(c)}(u)$ via $\alpha^{(d)}(u)$. So our verification methodology is as below: we simulate a discrete-time system shown in Fig. 1 and simulate a discrete-time Rayleigh fading channel with specified Doppler spectrum; given measurements from the queue, we can obtain the measured EC function, denoted by $\alpha_s(u)$, by the algorithm in Ref. [1, page 636]; since we have the analytical form for the discrete-frequency power spectral density $S(f_i)$, we can compute $\alpha^{(d)}(u)$ via (9). If $\alpha^{(d)}(u) \approx \alpha_s(u)$, i.e., the analytical result agrees with the simulation result, we would claim that the simulation verifies that the EC formula (10) given in Ref. [1] is accurate.

Specifically, our verification methodology is given as below.

1) Simulate a discrete-time Rayleigh fading channel with specified discrete-frequency Doppler spectrum $S(f_i)$. If we use a first-order autoregressive (AR) model to generate a correlated Rayleigh fading channel, Doppler spectrum $S(f_i)$ can be analytically derived from the AR(1) model parameters. Eq. (30) in Section V-B.1 gives the formula for $S(f_i)$.
2) Simulate the communication system shown in Fig. 1, where the source rate μ is constant.
3) Collect the following measurements from the queueing system at the n-th sampling epoch ($n = 1, 2, \cdots, N_T$): $S(n)$ the indicator of whether a packets is in service ($S(n) \in \{0, 1\}$), $Q(n)$ the number of bits in the queue (excluding the packet in service), and $\tau(n)$ the remaining service time of the packet in service (if there is one in service).
4) Calculate the measured EC function $\alpha_s(u)$ by the following procedure.

$$\hat{\gamma} = \frac{1}{N_T} \sum_{t=1}^{N_T} S(n), \tag{11}$$

$$\hat{q} = \frac{1}{N_T} \sum_{t=1}^{N_T} Q(n), \tag{12}$$

$$\hat{\tau_s} = \frac{1}{N_T} \sum_{t=1}^{N_T} \tau(n), \tag{13}$$

$$\hat{\theta} = \frac{\hat{\gamma} \times \mu}{\mu \times \hat{\tau}_s + \hat{q}}, \tag{14}$$

$$\alpha_s(u) = \mu, \quad \text{for } u = \hat{\theta}/\mu. \tag{15}$$

5) Compute $\alpha^{(d)}(u)$ via (9), where f_m and $S(f_i)$ are known.

6) Verify whether the error $|\alpha^{(d)}(u) - \alpha_s(u)|$ is small.

We follow the above verification methodology and conduct simulations in Section V-B.1. As shown in Figs. 2 to 4, the curve for $\alpha^{(d)}(u)$ matches that for $\alpha_s(u)$. This verifies that the EC formula (9) is accurate; hence, the EC formula (10) given in Ref. [1] is accurate.

IV. Spectral-Estimation-Based Algorithm and Estimation Error Analysis

Now we know that the EC formulae (10) and (9) are accurate. The next question is how to use the EC formulae in practice.

Since practical systems are discrete-time systems, we need to use (9) instead of (10). Furthermore, we cannot directly use (9) to compute the EC function since the power spectral density of the fading channel is not given *a priori*; in other words, we need to estimate the power spectral density of the fading channel in order to use (9). Hence, to facilitate the application of the EC theory to the design of practical QoS provisioning mechanisms in wireless networks, we propose a spectral-estimation-based algorithm to estimate the EC function based on the new discrete-frequency EC formula (9), given channel measurements.

Algorithm 1: Estimating the EC function via spectral estimation:

1) Obtain N_f measurements of the channel gain over the duration $[0, t]$, spaced at a time-interval δ apart. Denote these measurements by $\mathbf{x} = [x(0), x(1), \cdots, x(N_f-1)]^T$, where $x(n)$ $(n = 0, 1, \cdots, N_f-1)$ are the complex-valued channel gains.

2) Given channel gain measurements $\mathbf{x}$, estimate the power spectral density $\{\hat{S}(f_i), i = 1, \cdots, N_f\}$ via a spectral estimation method such as periodogram, Burg's maximum entropy method, and Capon's filter bank method [12]. Note that usually a few hundred samples are enough for these spectral estimation methods [12] to obtain a relatively accurate $\{\hat{S}(f_i)\}$.

3) Denote the estimated EC function by $\hat{\alpha}_e(u)$. Given $\{\hat{S}(f_i)\}$, we estimate $\hat{\alpha}_e(u)$ by

$$\hat{\alpha}_e(u) = \frac{\sum_{i=1}^{N_f} \log(u\hat{S}(f_i)+1)\Delta f_s}{u} \tag{16}$$

where $\Delta f_s = 2 \times f_m/(N_f - 1)$ and f_m is the maximum Doppler frequency of the fading channel. ■

We implement Algorithm 1 and conduct simulations in Section V-B.2. As shown in Figs. 5 to 7, the curve for $\hat{\alpha}_e(u)$ agrees well with that for $\alpha^{(d)}(u)$. It is also observed that the smaller value of u, the larger the estimation error $|\alpha^{(d)}(u) - \hat{\alpha}_e(u)|$. This can be explained by the following proposition, which provides the estimation error analysis.

Proposition 1: Define the estimation error $\epsilon(u) = |\alpha^{(d)}(u) - \hat{\alpha}_e(u)|$ for $u > 0$.

1) $\epsilon(u) \leq \overline{\epsilon}(u)$, where

$$\overline{\epsilon}(u) = \sum_{i=1}^{N_f} \Delta f_s \left| \frac{1}{u} \log\left(\frac{S(f_i) + 1/u}{\hat{S}(f_i) + 1/u} \right) \right|. \tag{17}$$

2) $\overline{\epsilon}(u)$ is a monotonically decreasing function of u for $u > 0$.

3) $\sup_{u>0} \epsilon(u) \leq \lim_{u\to 0} \overline{\epsilon}(u)$ and $\lim_{u\to 0} \overline{\epsilon}(u) = \sum_{i=1}^{N_f} \left| [S(f_i) - \hat{S}(f_i)]\Delta f_s \right|$.

4) $\inf_{u>0} \epsilon(u) = \lim_{u\to\infty} \overline{\epsilon}(u) = 0$.

Proof: 1) We prove $\epsilon(u)$ is upper bounded by $\overline{\epsilon}(u)$.

$$\begin{aligned}
\epsilon(u) &= |\alpha^{(d)}(u) - \hat{\alpha}_e(u)| \\
&= \left| \frac{\sum_{i=1}^{N_f} \log(uS(f_i)+1)\Delta f_s}{u} - \frac{\sum_{i=1}^{N_f} \log(u\hat{S}(f_i)+1)\Delta f_s}{u} \right| \\
&= \Delta f_s \left| \frac{1}{u} \sum_{i=1}^{N_f} \log\left(\frac{uS(f_i)+1}{u\hat{S}(f_i)+1} \right) \right| \\
&= \Delta f_s \left| \frac{1}{u} \sum_{i=1}^{N_f} \log\left(\frac{S(f_i)+1/u}{\hat{S}(f_i)+1/u} \right) \right| \\
&\leq \Delta f_s \left(\sum_{i=1}^{N_f} \left| \frac{1}{u} \log\left(\frac{S(f_i)+1/u}{\hat{S}(f_i)+1/u} \right) \right| \right) = \overline{\epsilon}(u)
\end{aligned} \tag{18}$$

2) We prove that $\overline{\epsilon}(u)$ is a monotonically decreasing function of u for $u > 0$. We achieve this by proving each term in the sum of the right hand side of (17), i.e., $\left| \frac{1}{u} \log\left(\frac{S(f_i)+1/u}{\hat{S}(f_i)+1/u} \right) \right|$, is a monotonically decreasing function of u for $u > 0$. We first let $v = 1/u$. Since $S(f_i) \geq 0$ and $\hat{S}(f_i) \geq 0$, we only need to prove $\left| v \log(\frac{a+v}{b+v}) \right|$ is a monotonically increasing function of v for $v > 0$ and $a \geq 0$, $b \geq 0$. Now we prove this. First, to remove the operation of absolute value, we consider two cases as below.

$$\left|v\log(\frac{a+v}{b+v})\right| = \begin{cases} v\log(\frac{a+v}{b+v}), & \text{if } a > b \geq 0, v > 0, \\ v\log(\frac{b+v}{a+v}), & \text{if } 0 \leq a < b, v > 0. \end{cases}$$

Considering the two cases, it is obvious that we just need to prove $v\log(\frac{a+v}{b+v})$ is a monotonically increasing function of v for $v > 0, a > b \geq 0$, which implies that $\left|v\log(\frac{a+v}{b+v})\right|$ is a monotonically increasing function of v for $v > 0$ and $a \geq 0$, $b \geq 0$. To prove this, we just need to show its derivative is non-negative. Define $f(v) = v\log(\frac{a+v}{b+v})$. Then, we prove its derivative $f'(v) \geq 0$ as below

$$\begin{aligned} f'(v) &= \log(\frac{a+v}{b+v}) - \frac{(a-b)v}{(a+v)(b+v)} \\ &= \log(\frac{1+a/v}{1+b/v}) - \frac{(a/v - b/v)}{(1+a/v)(1+b/v)} \\ &\overset{(a)}{\geq} 1 - \frac{1+b/v}{1+a/v} - \frac{(a/v-b/v)}{(1+a/v)(1+b/v)} \\ &= \frac{b(a-b)}{(a+v)(b+v)} \\ &\overset{(b)}{\geq} 0 \end{aligned} \tag{20}$$

where (a) is due to $\log(1/x) \geq 1 - x$ for $x > 0$, and (b) due to $v > 0, a > b \geq 0$.

3) We prove $\sup_{u>0}\epsilon(u) \leq \lim_{u\to 0}\overline{\epsilon}(u)$ and $\lim_{u\to 0}\overline{\epsilon}(u) = \sum_{i=1}^{N_f}\left|[S(f_i) - \hat{S}(f_i)]\Delta f_s\right|$ as below.

$$\begin{aligned} \sup_{u>0}\epsilon(u) &\overset{(a)}{\leq} \sup_{u>0}\overline{\epsilon}(u) \\ &\overset{(b)}{=} \lim_{u\to 0}\overline{\epsilon}(u) \\ &= \lim_{u\to 0}\Delta f_s\sum_{i=1}^{N_f}\left|\{\log[(uS(f_i)+1)^{\frac{1}{u}}] - \log[(u\hat{S}(f_i)+1)^{\frac{1}{u}}]\}\right| \\ &= \Delta f_s\sum_{i=1}^{N_f}\left|\lim_{u\to 0}\{\log[(uS(f_i)+1)^{\frac{1}{u}}] - \log[(u\hat{S}(f_i)+1)^{\frac{1}{u}}]\}\right| \\ &\overset{(c)}{=} \Delta f_s\sum_{i=1}^{N_f}\left|\{\log(e^{S(f_i)}) - \log(e^{\hat{S}(f_i)})\}\right| \\ &= \sum_{i=1}^{N_f}\left|[S(f_i) - \hat{S}(f_i)]\Delta f_s\right| \end{aligned} \tag{21}$$

where (a) follows from the fact that $\epsilon(u) \leq \overline{\epsilon}(u)$ and both $\epsilon(u)$ and $\overline{\epsilon}(u)$ are continuous functions, (b) due to the fact that $\overline{\epsilon}(u)$ is a monotonically decreasing function of u for $u > 0$, and (c) from $\lim_{x\to 0}(1+x)^{\frac{1}{x}} = e$.

4) To prove $\inf_{u>0}\epsilon(u) = \lim_{u\to\infty}\overline{\epsilon}(u) = 0$, we first prove $\inf_{u>0}\epsilon(u) \leq \lim_{u\to\infty}\overline{\epsilon}(u) = 0$ as below and then prove $\inf_{u>0}\epsilon(u) \geq 0$.

$$\begin{aligned}
\inf_{u>0}\epsilon(u) &\overset{(a)}{\leq} \inf_{u>0}\overline{\epsilon}(u) \\
&\overset{(b)}{=} \lim_{u\to\infty}\overline{\epsilon}(u) \\
&= \lim_{u\to\infty}\Delta f_s\sum_{i=1}^{N_f}\left|\frac{1}{u}\log\left(\frac{uS(f_i)+1}{u\hat{S}(f_i)+1}\right)\right| \\
&\overset{(c)}{=} \lim_{v\to 0}\Delta f_s\sum_{i=1}^{N_f}\left|v\log\left(\frac{S(f_i)+v}{\hat{S}(f_i)+v}\right)\right| \\
&= 0
\end{aligned} \tag{22}$$

where (a) follows from the fact that $\epsilon(u) \leq \overline{\epsilon}(u)$ and both $\epsilon(u)$ and $\overline{\epsilon}(u)$ are continuous functions, (b) due to the fact that $\overline{\epsilon}(u)$ is a monotonically decreasing function of u for $u > 0$, and (c) due to $v = 1/u$. On the other hand, since $\epsilon(u) = |\alpha^{(d)}(u) - \hat{\alpha}_e(u)| \geq 0$ for $u > 0$ and $\epsilon(u)$ is a continuous function, hence $\inf_{u>0}\epsilon(u) \geq 0$. Combining this with (22), we have $\inf_{u>0}\epsilon(u) = 0$. ■

From Proposition 1, we know that $\overline{\epsilon}(u)$ is a monotonically decreasing function of u for $u > 0$. This is why the simulation results show that the smaller value of u, the larger the estimation error $|\alpha^{(d)}(u) - \hat{\alpha}_e(u)|$. Proposition 1 also states that $\inf_{u>0}\epsilon(u) = \lim_{u\to\infty}\overline{\epsilon}(u) = 0$, i.e., $\overline{\epsilon}(u) \to 0$ as $u \to \infty$. This explains our observation from the simulation results that the estimation error diminishes as u increases.

From (17), since N_f is finite and the values of $S(f_i)$ and $\hat{S}(f_i)$ are finite, hence $\overline{\epsilon}(u)$ is upper bounded, i.e., $\epsilon(u)$ is also upper bounded.

V. Simulation Results

A. Simulation Setting

We simulate the discrete-time system depicted in Fig. 1. In this system, the data source generates packets at a *constant* rate μ. Generated packets are first sent to the (infinite) buffer at the transmitter, whose queue length is $Q(n)$, where n refers to the n-th sample-interval. The head-of-line packet in the queue is transmitted over the fading channel at data rate $r(n)$. The fading channel has a random power gain $g(n)$. We use a fluid model, that is, the size of a packet is infinitesimal. In practical systems, the results presented here will have to be modified to account for finite packet sizes.

We assume that the transmitter has perfect knowledge of the current channel gains $g(n)$ at each sample-interval. Therefore, it can use rate-adaptive transmissions and ideal channel codes, to transmit packets

without decoding errors. Thus, the transmission rate $r(n)$ is equal to the instantaneous (time-varying) capacity of the fading channel, as below,

$$r(n) = B_c \log_2(1 + g(n) \times P_0/\sigma_n^2) \tag{23}$$

where B_c denotes the channel bandwidth, and the transmission power P_0 and noise variance σ_n^2 are assumed to be constant. The average SNR is fixed in each simulation run and the average SNR $SNR_{avg} = E[g(n) \times P_0/\sigma^2]$. Since we set $E[g(n)] = 1$, we have $SNR_{avg} = E[g(n) \times P_0/\sigma^2] = P_0/\sigma^2$.

In our simulations, the sampling interval δ is set to 1 milli-second. This is not too far from reality, since 3G WCDMA systems already incorporate rate adaptation on the order of 10 milli-second [13]. Meanwhile, for the current enhanced HSPA systems, they have much faster adaptation speed, i.e. on the order of 2 milli-second.

Each simulation run is 10,000-second long for all the scenarios, in order to obtain good estimate by the Monte Carlo method. Since the sampling interval is 1 milli-second, we have 10,000,000 samples for estimation.

Denote $h(n)$ the voltage gain in the n^{th} sample interval. We generate Rayleigh flat-fading voltage-gains $h(n)$ by a first-order auto-regressive (AR(1)) model as below. We first generate $\bar{h}(n)$ by

$$\bar{h}(n) = \kappa \times \bar{h}(n-1) + u_g(n), \tag{24}$$

where $u_g(n)$ are i.i.d. complex Gaussian variables with zero mean and unity variance per dimension. Then, we normalize $\bar{h}(n)$ and obtain $h(n)$ by

$$h(n) = \bar{h}(n)/\sqrt{\frac{2}{1-\kappa^2}} = \bar{h}(n) \times \sqrt{\frac{1-\kappa^2}{2}}. \tag{25}$$

It is clear that (25) results in $E[g(n)] = E[|h(n)|^2] = 1$. The coefficient κ determines the Doppler frequency, *i.e.*, the larger the κ, the smaller the Doppler frequency. Specifically, the coefficient κ can be determined by the following procedure: 1) compute the coherence time T_c by [14, page 165]

$$T_c \approx \frac{9}{16\pi f_m}, \tag{26}$$

where the coherence time is defined as the time, over which the time auto-correlation function of the fading process is above 0.5; 2) compute the coefficient κ by[1]

$$\kappa = 0.5^{\delta/T_c}. \tag{27}$$

TABLE I

SIMULATION PARAMETERS.

Maximum Doppler frequency f_m	15/100/200 Hz
Channel bandwidth B_c	100 kHz
Average SNR	5/10/15 dB
Sampling-interval δ	1 ms
Number of samples N_f	1024

Table I lists the parameters used in our simulations.

B. Simulation Results

1) Verification of the EC Formula of Wu and Negi: We follow the verification methodology presented in Section III and conduct simulations in this section.

Since we use AR(1) model to generate a correlated Rayleigh fading channel, Doppler spectrum $S(f_i)$ can be analytically derived from the AR(1) model parameters as below. It is easy to prove that the Doppler spectrum of $\bar{h}(n)$ defined in (24) is given by

$$S_{\bar{h}}(f_i) = \frac{\sigma_{u_g}^2}{|1-\kappa e^{-j2\pi f_i}|^2}, \tag{28}$$

where $\sigma_{u_g}^2$ is the variance of $u_g(n)$; $|x|^2$ is the squared magnitude of complex number x. Since $h(n)$ in (25) is a normalized version of $\bar{h}(n)$, the Doppler spectrum of $h(n)$ is given by

$$S_h(f_i) = \frac{\frac{\sigma_{u_g}^2}{|1-\kappa e^{-j2\pi f_i}|^2}}{\sum_k \frac{\sigma_{u_g}^2}{|1-\kappa e^{-j2\pi f_k}|^2}} = \frac{1}{\sum_k \frac{|1-\kappa e^{-j2\pi f_i}|^2}{|1-\kappa e^{-j2\pi f_k}|^2}}, \tag{29}$$

which satisfies $\sum_i S_h(f_i) = E[|h(n)|^2] = 1$. Since $E[g(n)] = E[|h(n)|^2] = 1$ and $SNR_{avg} = E[g(n) \times P_0/\sigma^2] = P_0/\sigma^2$, then $S(f_i)$ is given by

$$S(f_i) = \frac{SNR_{avg}}{\sum_k \frac{|1-\kappa e^{-j2\pi f_i}|^2}{|1-\kappa e^{-j2\pi f_k}|^2}}, \tag{30}$$

which satisfies $\sum_i S(f_i) = SNR_{avg}$.

Figs. 2 to 4 show the measured EC function $\alpha_s(u)$ obtained from the simulation, and the discrete-form EC function $\alpha^{(d)}(u)$ obtained from analysis, under different Doppler frequency and different average SNR. It is observed that the curve for $\alpha^{(d)}(u)$ gives good agreement with that for $\alpha_s(u)$. The difference between $\alpha^{(d)}(u)$ and $\alpha_s(u)$ is mainly caused by the approximation in our analysis, i.e., $\log(1+|x|^2) \approx |x|^2$. The

[1]The auto-correlation function of the AR(1) process is κ^m, where m is the number of sample intervals. Solving $\kappa^{T_c/\delta} = 0.5$ for κ, we obtain (27).

results in Figs. 2 to 4 verify that the EC formula (9) is accurate; hence, the EC formula (10) given in Ref. [1] is accurate.

From Figs. 2 to 4, we observe that the effective capacity $\alpha(u)$ decreases with the increase of Doppler frequency, for the same value of u. This can be explained as below. As we know [1], the larger Doppler frequency, the higher degree of time diversity. This translates to a larger μ for the same $\theta(\mu)$. Since $\theta = \mu \times u$, hence, for fixed QoS requirement θ, a larger μ indicates a smaller u. Hence, the increase of Doppler frequency leads to a decrease in u. Hence, we should not compare the effective capacity $\alpha(u)$ of different Doppler frequency, for the same value of u. If we examine the function $\mu(\theta)$, simulation results [1] show that for the same QoS requirement θ, a larger Doppler frequency results in a larger throughput μ.

2) Accuracy of Our Proposed Spectral-estimation-based EC Estimation Algorithm: We implement Algorithm 1 and conduct simulations in this section.

Figs. 5 to 7 show the estimated EC function $\hat{\alpha}_e(u)$ obtained from the simulation and estimation, and the discrete-form EC function $\alpha^{(d)}(u)$ obtained from analysis, under different Doppler frequency and different average SNR. It can be observed that the curves for $\alpha^{(d)}(u)$ and $\hat{\alpha}_e(u)$ are very well matched. We also observe that the smaller value of u, the larger the estimation error $|\alpha^{(d)}(u) - \hat{\alpha}_e(u)|$. This is consistent with the estimation error analysis provided in Proposition 1.

The simulation results demonstrate that the estimated EC function by our algorithm is accurate enough so that one can apply the EC technique to the design of practical QoS provisioning mechanisms.

VI. Conclusions

In this work, we studied the accuracy of Wu and Negi's EC formula for a correlated Rayleigh fading channel. Through simulation, we confirmed that the EC formula of Wu and Negi is accurate. In practice, we cannot directly use the EC formula to compute the effective capacity since the power spectral density of the fading channel is not given *a priori*. To address this, we proposed a spectral-estimation-based algorithm to estimate the EC function, given channel measurements. In addition, we analyzed the effect of spectral estimation error on the accuracy of EC estimation. Simulation results showed that our proposed spectral-estimation-based EC estimation algorithm is accurate, indicating the excellent practicality of our algorithm.

The implication of this work is significant. Due to lack of (verified) closed-form EC formula for non-i.i.d. Rayleigh fading channels, most previous works only focus on i.i.d. Rayleigh fading channels. Now, we have verified that the EC formula of Wu and Negi is accurate; this allows researchers to use the EC formula to analyze and design communication systems under non-i.i.d. Rayleigh fading channels, instead of i.i.d. Rayleigh fading channels only. More importantly, our spectral-estimation-based EC estimation algorithm is shown to be accurate, which significantly facilitates the application of the EC theory to the design of practical QoS provisioning mechanisms in wireless networks.

ACKNOWLEDGMENT

This work was supported in part by the US National Science Foundation under grant CNS-0643731, the US Office of Naval Research under grant N000140810873, NSFC/RGC Joint Research Scheme No. 60831160524 and the open research fund of National Mobile Communications Research Laboratory, Southeast University, China.

REFERENCES

[1] D. Wu and R. Negi, "Effective capacity: a wireless link model for support of quality of service," *IEEE Transactions on wireless communications*, vol. 2, no. 4, pp. 630–643, 2003.

[2] C. Chang and J. Thomas, "Effective bandwidth in high-speed digital networks," *IEEE Journal on Selected areas in Communications*, vol. 13, no. 6, pp. 1091–1100, 1995.

[3] J. Tang and X. Zhang, "Quality-of-service driven power and rate adaptation for multichannel communications over wireless links," *IEEE Transactions on Wireless Communications*, vol. 6, no. 12, p. 4349, 2007.

[4] X. Zhang, J. Tang, H. Chen, S. Ci, and M. Guizani, "Cross-layer-based modeling for quality of service guarantees in mobile wireless networks," *IEEE Communications Magazine*, vol. 44, no. 1, pp. 100–106, 2006.

[5] J. Tang and X. Zhang, "Cross-layer resource allocation over wireless relay networks for quality of service provisioning," *IEEE Journal on Selected Areas in Communications*, vol. 25, no. 4, pp. 645–656, 2007.

[6] ——, "Cross-layer-model based adaptive resource allocation for statistical QoS guarantees in mobile wireless networks," *IEEE Transactions on Wireless Communications*, vol. 7, no. 6, pp. 2318–2328, 2008.

[7] C. Li, H. Che, and S. Li, "A wireless channel capacity model for quality of service," *IEEE Transactions on Wireless Communications*, vol. 6, no. 1, pp. 356–366, 2007.

[8] D. Park and B. Lee, "QoS Support by using CDF-based wireless packet scheduling in fading channels," *IEEE Transactions on Communications*, vol. 54, no. 11, pp. 2051–2061, 2006.

[9] W. Kumwilaisak, Y. Hou, Q. Zhang, W. Zhu, C. Kuo, and Y. Zhang, "A cross-layer quality-of-service mapping architecture for video delivery in wireless networks," *IEEE Journal on Selected Areas in Communications*, vol. 21, no. 10, pp. 1685–1698, 2003.

[10] L. Liu, P. Parag, J. Tang, W. Chen, and J. Chamberland, "Resource allocation and quality of service evaluation for wireless communication systems using fluid models," *IEEE Transactions on Information Theory*, vol. 53, no. 5, pp. 1767–1777, 2007.

[11] Y. Chen, J. Chen, and Y. Yang, "Multi-hop delay performance in wireless mesh networks," *Mob. Netw. Appl.*, vol. 13, no. 1-2, pp. 160–168, 2008.

[12] P. Stoica and R. Moses, *Spectral analysis of signals*. Pearson Prentice Hall, 2005.

[13] H. Holma and A. Toskala, *WCDMA for UMTS: Radio access for third generation mobile communications*. John Wiley & Sons, Inc. New York, NY, USA, 2000.

[14] T. Rappaport, *Wireless communications: principles and practice*. Prentice Hall PTR Upper Saddle River, NJ, USA, 2001.

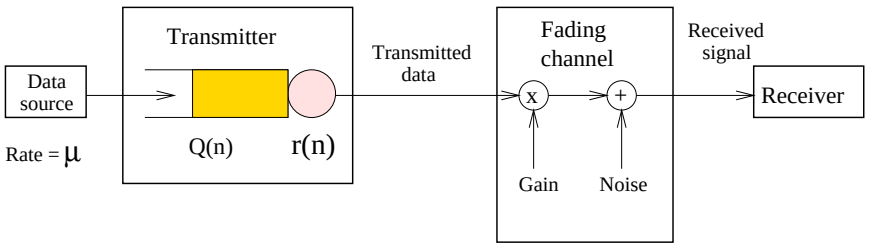

Fig. 1. The queueing system model.

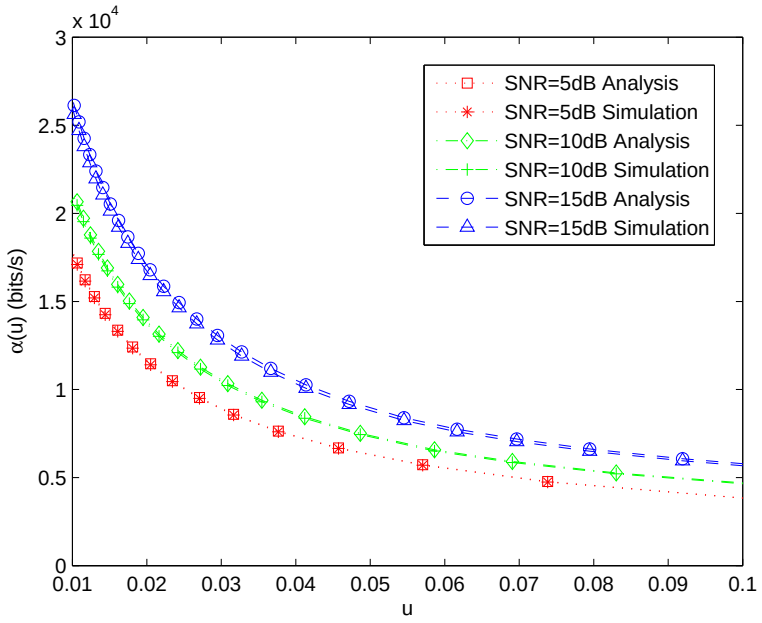

Fig. 2. $\alpha^{(d)}(u)$ (analysis) vs. $\alpha_s(u)$ (simulation) for Doppler frequency $f_m = 15$ Hz.

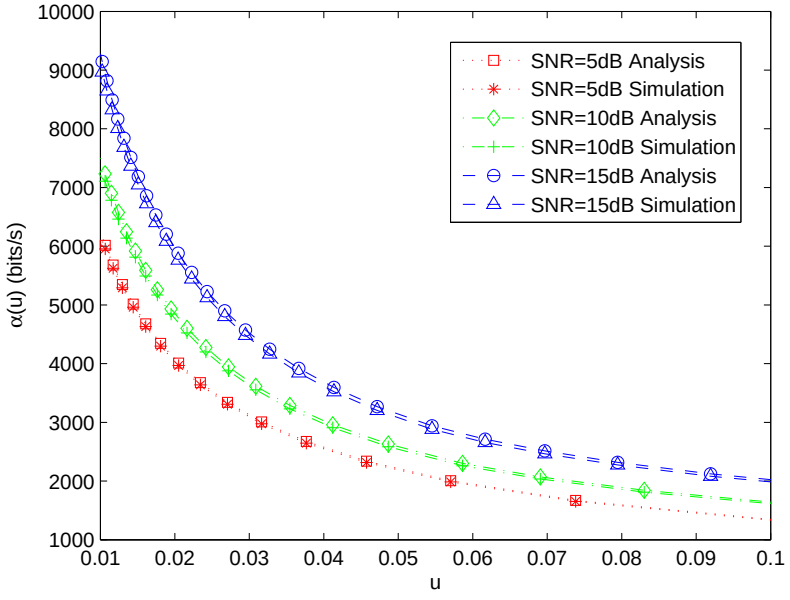

Fig. 3. $\alpha^{(d)}(u)$ (analysis) vs. $\alpha_s(u)$ (simulation) for Doppler frequency $f_m = 100$ Hz.

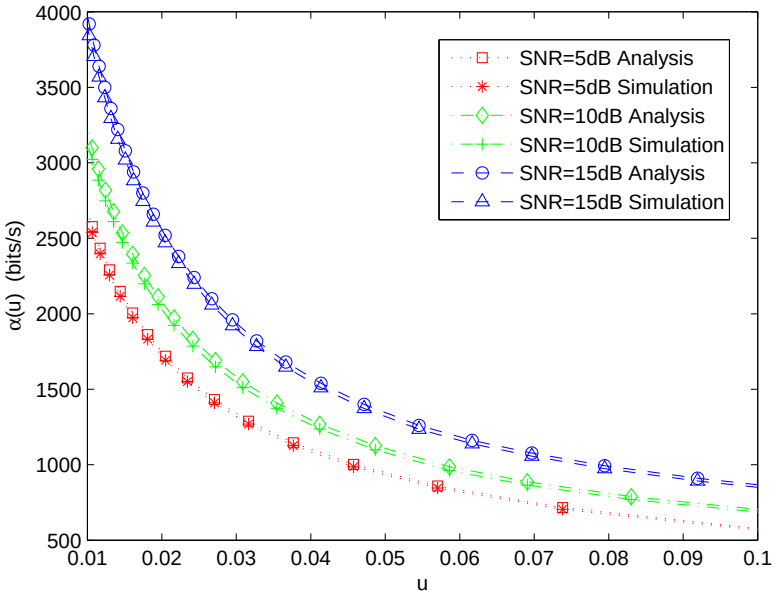

Fig. 4. $\alpha^{(d)}(u)$ (analysis) vs. $\alpha_s(u)$ (simulation) for Doppler frequency $f_m = 200$ Hz.

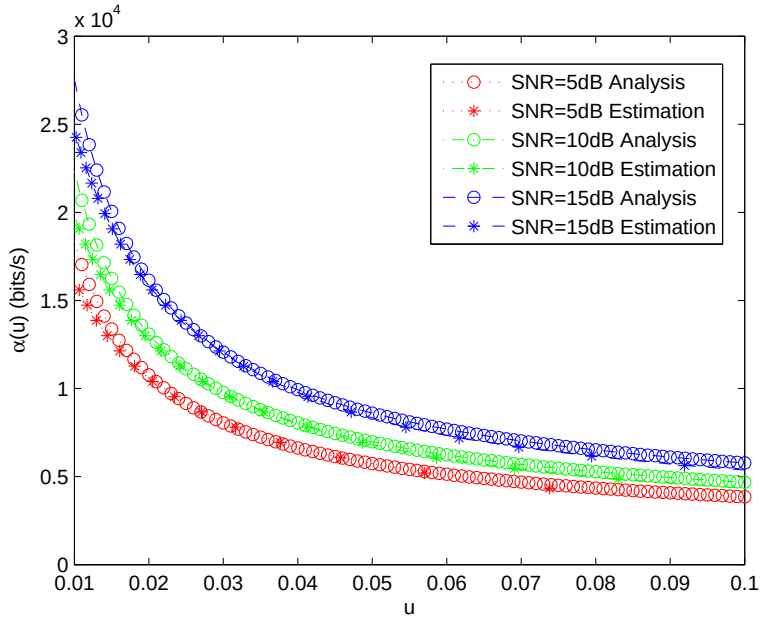

Fig. 5. $\alpha^{(d)}(u)$ (analysis) vs. $\hat{\alpha}_e(u)$ (estimation) for Doppler frequency $f_m = 15$ Hz.

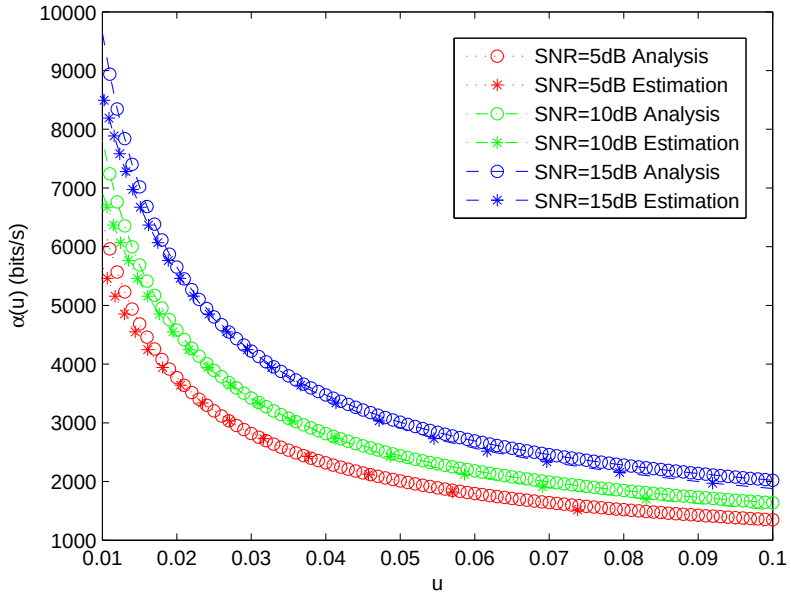

Fig. 6. $\alpha^{(d)}(u)$ (analysis) vs. $\hat{\alpha}_e(u)$ (estimation) for Doppler frequency $f_m = 100$ Hz.

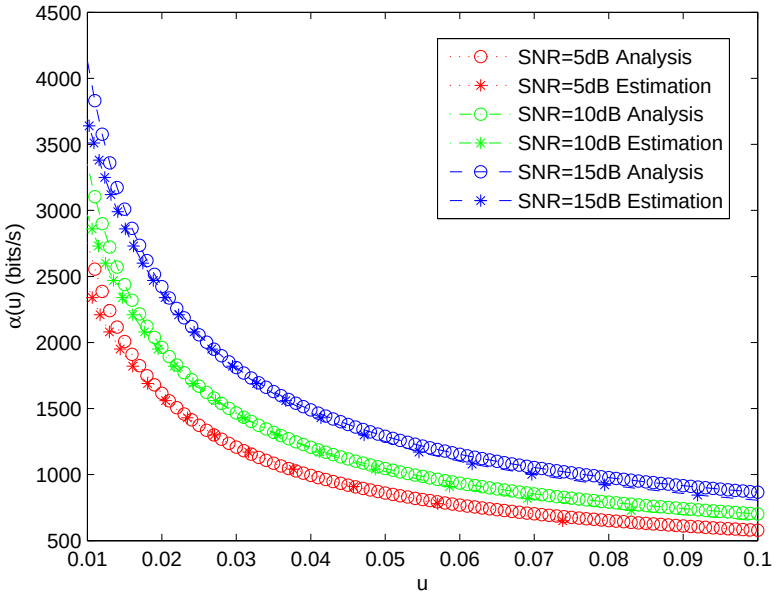

Fig. 7. $\alpha^{(d)}(u)$ (analysis) vs. $\hat{\alpha}_e(u)$ (estimation) for Doppler frequency $f_m = 200$ Hz.